Cement and Concrete Research 39 (2009) 989–996

Contents lists available at ScienceDirect

Cement and Concrete Research

journal homepage: http://ees.elsevier.com/CEMCON/default.asp

Early C_3A hydration in the presence of different kinds of calcium sulfate

S. Pourchet [a,*], L. Regnaud [b], J.P. Perez [c], A. Nonat [a]

[a] Institut Carnot de Bourgogne, UMR 5209 CNRS, Université de Bourgogne, 9 Av. A. Savary, BP 47 870, F-21078 DIJON Cedex, France
[b] Chryso , 7 rue de l'Europe, Zone Industrielle, 45300 Sermaises , France
[c] LCR Lafarge, 95 rue Montmurier, 38070 St Quentin Fallavier, France

ARTICLE INFO

Article history:
Received 22 April 2009
Accepted 21 July 2009

Keywords:
Hydration (A)
$Ca_3Al_2O_6$ (D)
Ettringite (D)
Kinetics (A)

ABSTRACT

Hydration reactions of C_3A with various amounts of calcium sulfate hemihydrate, gypsum or a mixture of the two, were investigated by isothermal microcalorimetry, and a monitoring of the ionic concentrations of diluted suspensions. This study shows that sulfate type used modifies the early C_3A–$CaSO_4$ hydration products and the rate of this hydration. The fast initial AFm formation observed before ettringite precipitation in the C_3A–gypsum system is avoided as soon as hemihydrate is present in the suspension. This was attributed to higher super saturation degrees and then higher nucleation frequency with regard to the ettringite obtained in the presence of hemihydrate. Moreover, replacement of gypsum by hemihydrate also leads to an increase of the ettringite formation rate during at least the five first hours under experimental conditions.

1. Introduction

Tricalcium aluminate, C_3A, is known to be the most reactive mineral present in Portland clinker. Its early hydration leads to the formation of calcium hydroaluminate ($3CaO–Al_2O_3–Ca(OH)_2–nH_2O$ or hydroxy–AFm) which induces a stiffening of the hydrating paste. In order to prevent this phenomenon, calcium sulfate is added to the clinker to slow down the early C_3A hydration, which then leads to the formation of ettringite ($Ca_6Al_3(SO_4)_3(OH)_{12}$, $26H_2O$) [1]. Because the liquid phase composition in this system is at early ages usually saturated or supersaturated with respect to gypsum, thermodynamic calculations show that ettringite should be the initial hydrate formed during hydration of C_3A–$CaSO_4$ mixtures at room temperature. However, prior work has shown that the hydroxy–AFm can also be formed during this step. Brown et al. [2] showed that C_3A hydration carried out in different solutions containing various amounts of sodium, calcium, hydroxide and sulfate ions gives rise to at least two hydrated phases (ettringite and hydroxy–AFm) precipitating in the same time, the proportions and the rate of precipitation of each phase depending on the composition of the solution. These findings are also in good accordance with the work of Eitel [3] showing hexagonal hydrate phases precipitating in direct contact with C_3A. More recently, Minard et al. [4] confirmed the formation of both ettringite and hydroxy–AFm at early ages in C_3A–gypsum hydration and determined the quantity of hydroaluminate precipitating by using a method based on microcalorimetry in stirred diluted suspension.

Even if the factors which control the kinetics of the hydration of C_3A–$CaSO_4$ mixtures are still under discussion [2,4–8] nevertheless most authors conclude that the initial rate of C_3A hydration is significantly influenced by the type of sulfate source used [5,9,10]. This is interpreted as a consequence of the solubility and the rate of dissolution of the particular form of calcium sulfates used. For example, Bensted [9] showed that increasing the grinding temperature of a Portland cement made with gypsum results in increased quantities of ettringite determined by DTA at all the hydration times examined up to 2 h. He attributed this effect to the increased solubility rate of the calcium sulfate, because when gypsum, is interground with clinker to produce cement, some of the gypsum can dehydrate to hemihydrate, depending on the temperature and humidity conditions. Hemihydrate has a higher solubility and solubility rate than gypsum, so a higher initial calcium sulfate concentration is expected in the pore fluid when gypsum is partially dehydrated to hemihydrate, and this could induce an increase of the ettringite precipitation rate.

Because early C_3A hydration is known to have a significant influence on the rheological properties of Portland cement pastes, and thus of concrete, it is of great interest to have a better understanding of this phenomenon. The purpose of this study is to examine how the nature of the calcium sulfate used (gypsum, hemihydrate, or a mixture of the two) can influence early C_3A hydration reactions, and more specifically, if it affects AFm formation. This work is based on calorimetry of stirred dilute C_3A suspensions, using Minard's procedure [4]. Using stirred suspensions instead of paste avoids possible heterogeneities in the mixture and decreases the concentration gradients at the interface between solids and aqueous phase. Moreover this method allows for quantification of the hydroaluminate formed at the very beginning. Parallel experiments were carried out in thermoregulated reactors allowing frequent

* Corresponding author.
E-mail address: sylvie.pourchet@u-bourgogne.fr (S. Pourchet).

0008-8846/$ – see front matter © 2009 Elsevier Ltd. All rights reserved.
doi:10.1016/j.cemconres.2009.07.019

sampling of solid and liquid for analysis. Results are discussed by considering the effect of the type of calcium sulfate used on the pore solution composition.

2. Materials and methods

2.1. Materials

Most of the experiments were made with the same batch of cubic C_3A. Its specific surface area determined by Blaine's method was 370 m^2/kg and its particle size distribution is depicted below (Fig. 1). Another batch of cubic C_3A was used for supplementary experiments led in the presence of ettringite. In this case its specific area determined by Blaine's method was 330 m^2/kg. Both were supplied by Lafarge LCR.

As calcium sulfate sources, gypsum (RP Normapur, Merck) and pure hemihydrate (Fluka) were used. Ettringite was synthesized by Lafarge according to [11] and analysed by XRD.

2.2. Methods

2.2.1. Heat evolution rate in diluted suspension

The hydration of C_3A was followed at 25 °C with a high sensitivity (0.1 μW) isothermal Tian–Calvet microcalorimeter in diluted suspension (Setaram, M60, and Setaram MS80). A tube with a calorimetric cell as presented in Fig. 2 is introduced in the calorimeter which transmits the heat evolution. C_3A hydration was studied in a portlandite saturated solution in order to mimic the pore solution during early cement hydration. Then for the experiments, 50 mL of a saturated calcium hydroxide solution were introduced into the cell, and 2 g of C_3A placed in the tank. When C_3A hydration was carried out with gypsum, the appropriate amount of solid gypsum was either introduced in the cell with the solution or dry-mixed with C_3A in a turbula mixer and this mix was then placed in the tank. In the case of hemihydrate–C_3A hydration, hemihydrate was first dry-mixed with C_3A, in order to avoid the hydration of hemihydrate into gypsum before the introduction of C_3A in the cell. This mix was then placed in the tank. In the case of the C_3A–ettringite–gypsum hydration experiment, 0.2 g of ettringite was added to the initial gypsum suspension.

To begin each experiment, the calorimetric tube was introduced in the calorimeter and the agitation of the solution begun. Once the thermal equilibrium was reached (after about 4 h), C_3A (respectively C_3A + hemihydrate, or C_3A + gypsum) was introduced into the cell from the tank, and the heat evolution rate was then registered as a function of time.

A typical heat evolution rate curve recorded during the hydration of C_3A–gypsum mix (20% by weight related to the C_3A) is shown in Fig. 3.

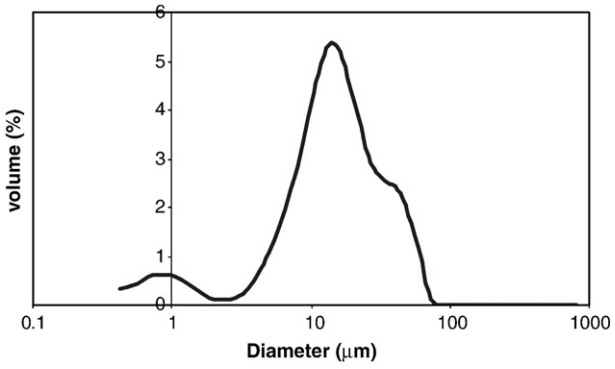

Fig. 1. Particle size distribution of C_3A determined in ethanol by laser light scattering.

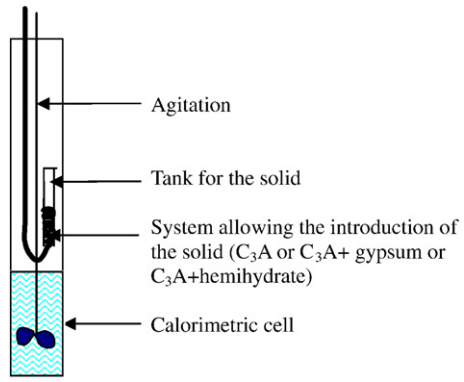

Fig. 2. Schematic view of the calorimetric tube.

Two sharp exothermic peaks are visible on the heat evolution rate curve. The first one corresponds to dissolution of C_3A, precipitation of AFm and beginning of precipitation of ettringite [4,12,13]. Dissolution of C_3A and precipitation of ettringite continue simultaneously at the same rate until the second sharp exothermic peak appears. This one occurs as soon as the calcium sulfate is depleted [4,12,13].

2.2.2. Determination of the amount of AFm precipitated at early age

The basis of the method is described in [4]. The cumulated heat between $t = 0$ and the time of appearance of the second sharp peak corresponds to the heat released by the formation of AFm and ettringite from C_3A hydration. Varying the amount of calcium sulfate varies the amount of ettringite in the same proportion as well. The plot of this cumulated heat versus the amount of the calcium sulfate initially added (expressed in mole number) leads to a straight line the slope of which is the molar heat of formation of ettringite from C_3A and calcium sulfate and the y-intercept is the total heat released by the formation of AFm from C_3A.

2.2.3. Measurement of ion concentrations during hydration and analysis of the product

The same experiments as those performed in the calorimeter were carried out in a thermoregulated (25 °C) reactor. The $C_3A/CaSO_4$ mixture was also hydrated in a (initially) portlandite saturated suspension, under inert atmosphere in order to avoid carbonation, with a liquid to C_3A ratio of 25 (10 g of C_3A in 250 ml of solution). The suspension was continuously stirred with a mechanical stirrer. Calcium, aluminium and sulfate concentrations of the solution were determined by Atomic Emission Spectrometry (ICP-OES) after a 0.3 μm filtration. Hydrochloric acid was added to the samples in order to avoid carbonation.

In the same time a small portion of the suspension was filtered 5 min after the mixing, through 0.3 μm millipore filter, and then washed with

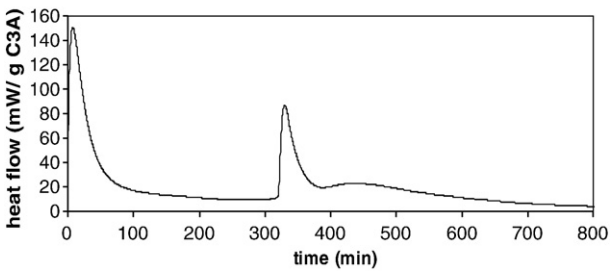

Fig. 3. Heat flow evolution over time during C_3A hydration in the presence of 20% gypsum (expressed by weight of C_3A) in a saturated calcium hydroxide solution L/S = 25.

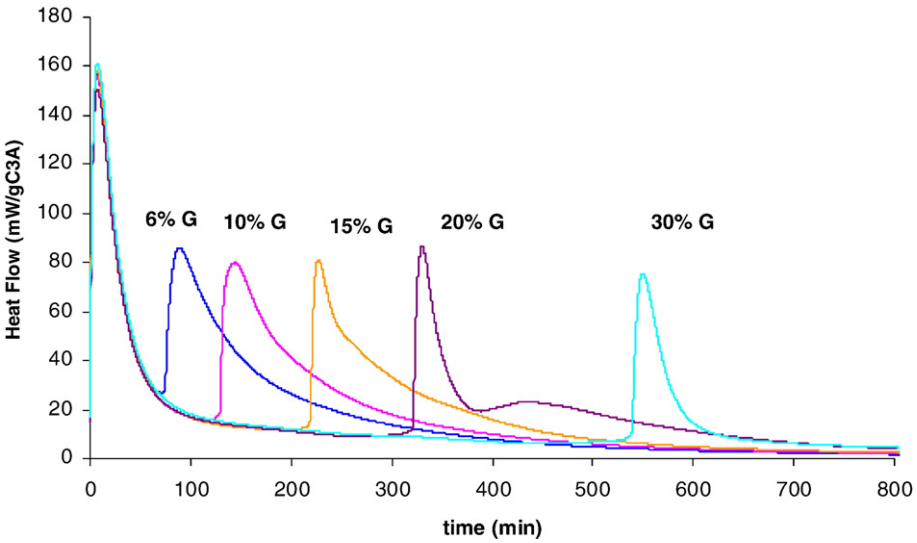

Fig. 4. Heat flow evolution over time during C_3A–gypsum hydration with different initial amount of gypsum (% by weight of C_3A) in saturated calcium hydroxide solution L/S = 25.

pure ethanol in order to analyse the solid product by SEM (Jeol, Model 6400F).

3. Results

3.1. Comparison of C_3A–gypsum and C_3A–hemihydrate hydrations

Various amounts of gypsum and hemihydrate (6 to 30% equivalent of gypsum by weight related to the C_3A amount) were added to C_3A and hydrated in stirred diluted suspensions. Heat evolution rate curves are reported in Figs. 4 and 5 respectively. Previous experiments have shown that heat evolution rate curves are the same whatever the gypsum addition (solid gypsum initially added to the initial solution or solid gypsum dry-mixed with C_3A).

The first exothermic peak is superimposable whatever the amount of gypsum or hemihydrate added, nevertheless it appears to be lower when C_3A hydrates in the presence of hemihydrate. Namely when the initial heat flow liberated per gram of C_3A corresponds to 160 mW in the case of the C_3A–gypsum hydration, the heat evolution rate curves obtained with the C_3A–hemihydrate show an initial heat flow of about 95 mW per gram of C_3A.

Furthermore the exothermic hydration of the hemihydrate into gypsum also gives rise to a significant exothermic peak which appears after about 70 min for the highest amounts of hemihydrate added. Because of the higher solubility of hemihydrate compared to gypsum, higher sulfate and calcium ions concentrations are observed within the first minutes (Fig. 7 vs Fig. 6). The solution quickly becomes supersaturated with respect to gypsum which nucleates and then precipitates giving rise to a decrease in the aqueous sulfate and calcium concentrations. Fig. 7 does not clearly show a concentration plateau corresponding to the gypsum solubility equilibrium point, maybe because the number of experimental points was not sufficient but more probably because the rate of growth of gypsum was too slow under these conditions, so that, by the time the gypsum solubility point was reached, there was no longer much gypsum left.

3.2. C_3A–gypsum–hemihydrate hydrations

For these experiments, we used a mix of gypsum and hemihydrate as sulfate source. 6% of gypsum by weight of C_3A (0.35 mmol/g C_3A) was introduced in the solution and we added different quantities of hemihydrate varying from 6 to 25% by weight of C_3A (corresponding to 7 to 30% equivalent gypsum related to C_3A weight).

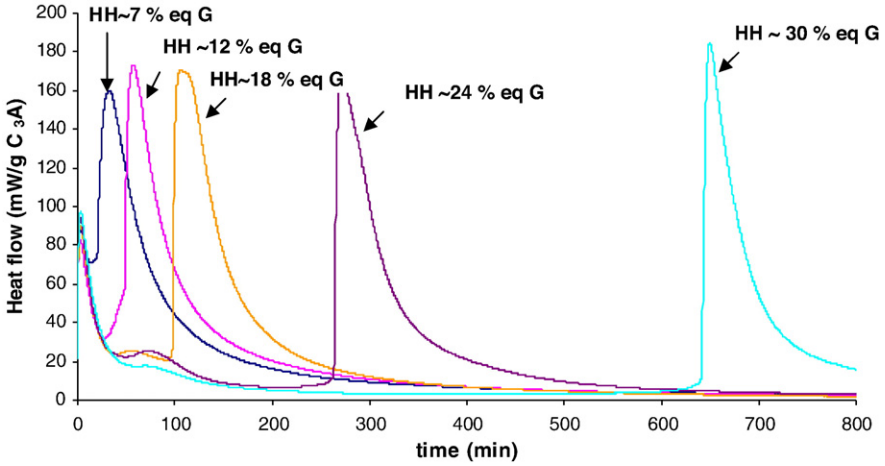

Fig. 5. Heat flow evolution over time during C_3A hydration in presence of different initial amount of hemihydrate (expressed as % of equivalent gypsum by weight of C_3A) in portlandite saturated solution L/S = 25.

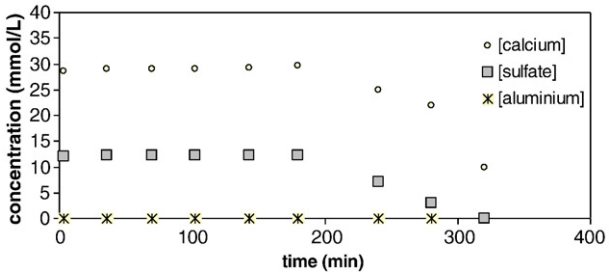

Fig. 6. Calcium and sulfate ions concentration vs. time during the C_3A–gypsum hydration (20% of gypsum by weight of C_3A) carried out in a calcium hydroxide saturated solution in a thermoregulated reactor (25 °C). (L/S = 25). The concentration plateau lasts as long as solid gypsum remains in equilibrium with its saturated solution. When the gypsum is depleted, the precipitation of ettringite continued as long as sulfate ions are still present in the solution. The total depletion of sulfate coincides with the appearance of the second exothermic peak [4].

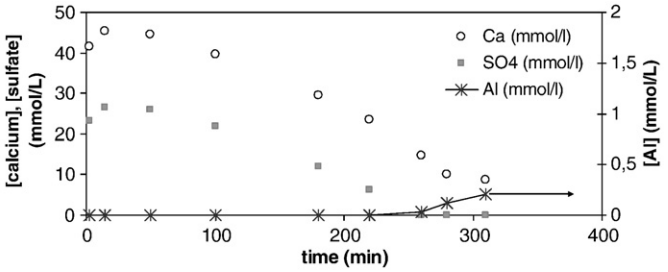

Fig. 7. Calcium, sulfate and aluminium ions concentration as a function of time during C_3A–hemihydrate hydration in a portlandite saturated and thermoregulated solution (L/S = 25). 20% of hemihydrate by weight of C_3A was added (equivalent ~24% gypsum).

The calorimetric curves reveal that the C_3A hydration in the presence of a mix of hemihydrate and gypsum seems to be similar to the hydration carried out in the presence of pure hemihydrate (Fig. 8). The intensity of the first exothermic peak is roughly the same as the intensity obtained in the presence of pure hemihydrate, with an intensity of about 90 mW/g C_3A.

The second low exothermic peak appearing within the first 200 min again results from the exothermic hydration of hemihydrate into gypsum.

3.3. Estimation of the amount of AFm initially-precipitated

Previous results allow to determine the total heat released when sulfate ions are depleted, by integrating the heat flow curves. This total heat is then reported as a function of the initial quantity of calcium sulfate added for the three studies (pure gypsum, pure hemihydrate and mix of them).

In the case of hemihydrate, the heat resulting from the hydration of hemihydrate into gypsum was deduced from the cumulated heat released at the exhaustion of sulfate. Fig. 9 shows that cumulated heat released at the depletion of sulfate is obviously linearly related to the number of added $CaSO_4$ mole whatever the type of calcium sulfate. Assuming that all consumed calcium sulfate is only used to precipitate ettringite, fitting the linear relationship allows to calculate the slope which is obviously directly connected to the ΔH of the resulting equation:

$$Ca_3Al_2O_6 + 3CaSO_4 + 32H_2O \rightarrow Ca_6Al_2(SO_4)_3(OH)_{12}, 26H_2O \quad (1)$$

As expected, the slope is the same, whatever the type of calcium sulfate. From these results we are able to experimentally determine the value of ΔH_{eqV} associated to the Eq. (1) in the three cases. We find $\Delta H_{eq\,I}$ equals to −636, −615 and −615 kJ/mol in the cases of gypsum, hemihydrate and the mix of both respectively, which is in the same order of magnitude as the value determined by Minard. (−600 kJ/mol).

The interesting point of this study concerns the *y*-intercept which is different according to the type of calcium sulfate. In the presence of hemihydrate or in the presence of a mix of hemihydrate and gypsum, the y-intercept is close to zero, but in presence of gypsum only, the *y*-intercept is equal to 260 J/g C_3A under the experimental conditions.

If we consider that only ettringite precipitates from the C_3A–gypsum hydration, the *y*-intercept of this curve should be close to zero as observed when hemihydrate is present. When C_3A hydrates in the presence of pure gypsum, the high value found for the *y*-intercept in the Fig. 9 confirmed that another exothermic "phenomenon" took place during the first part of the C_3A hydration, without consuming any sulfate ion. According to Minard et al. [4] this phenomenon is connected to the intensity of the first exothermic peak which mainly results from the C_3A dissolution giving rise to the very early hydroxyl–AFm precipitation.

Assuming a value of 800 J/g for the heat release during the exothermic hydration of 1 g of C_3A into AFm [13], under the conditions

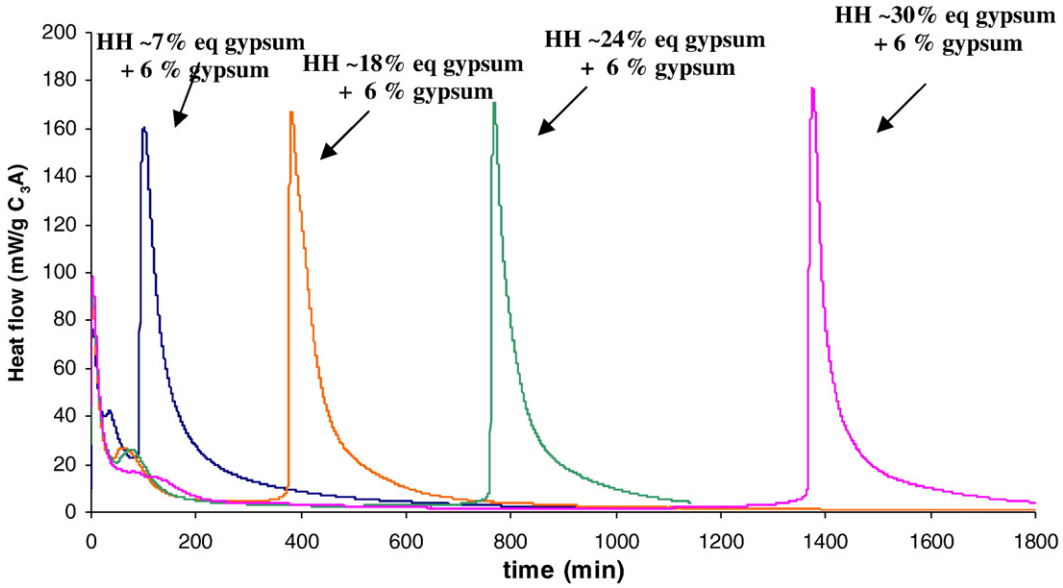

Fig. 8. Heat evolution rate curves over time during C_3A hydration in the presence of different initial amounts of hemihydrate (% by weight of C3A) and 6% by weight of C3A of gypsum in saturated Ca $(OH)_2$ solution L/S = 25.

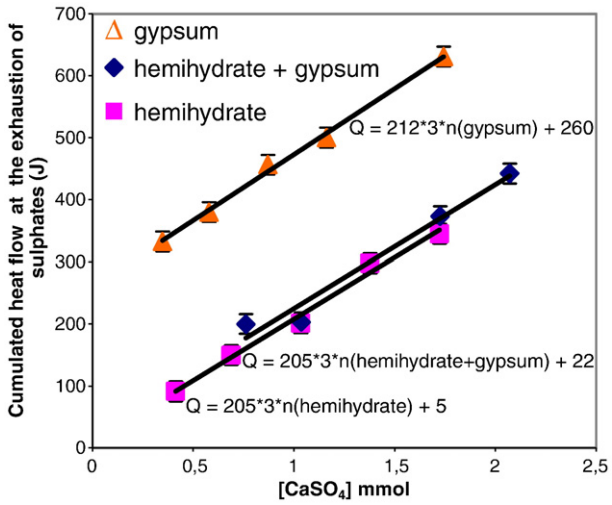

Fig. 9. Cumulative heat flow at the exhaustion of $CaSO_4$ as a function of the amount of $CaSO_4$ added when 1 g of C_3A is hydrated in 25 ml of an initially portlandite-saturated suspension.

of this study and with the C_3A used, we find that about 30% of the C_3A introduced might very quickly hydrate into AFm when C_3A hydrated in the presence of pure gypsum. In the presence of hemihydrate the early hydroxyl–AFm precipitation does not seems to occur. These assumptions are confirmed by S.E.M. micrography of a C_3A grain hydrated 5 min in saturated calcium hydroxide solution in presence of gypsum or hemihydrate respectively (Fig. 10): whereas the C_3A grain is covered by platelets of AFm when the hydration is carried out in the presence of gypsum, only small ettringite needles are observed on the C_3A grain hydrated in the presence of hemihydrate.

4. Discussion

4.1. Calculation of the super saturation degrees for the C_3A–calcium sulfate systems

When C_3A dissolves, it leads to ions in solution according to

$$Ca_3Al_2O_6 + H_2O \rightarrow 3Ca^{2+} + 2Al^{3+} + 12OH^-$$

and the solution becomes very fast supersaturated,

- with respect to hydroxyl–AFm which should precipitate according to

$$4Ca^{2+} + 2Al^{3+} + 12OH^- + 7H_2O = Ca_4Al_2(OH)_{12}, 7H_2O$$

and $Ks_{C4AH13} = (Ca^{2+})^4\,(Al^{3+})^2\,(OH^-)^{12}$ is the solubility product of C_4AH_{13}

- and with respect to ettringite if calcium sulfate is added, which also should precipitate according to

$$6Ca^{2+} + 2Al^{3+} + 12OH^- + 3SO_4^{2-} + 26H_2O = Ca_6Al_2(OH)_{12}(SO_4)_3 26H_2O$$

and $Ks_{ettringite} = (Ca^{2+})^6\,(Al^{3+})^2\,(OH^-)^{12}\,(SO_4^{2-})^3$ is the solubility product of ettringite.

Taking log $Ks_{C4AH13} = -103.76$ and log $Ks_{ettringite} = -55.19$ [14], we calculated the evolution of the saturation degrees of the solution with respect to both AFm and ettringite when C_3A continuously dissolves under experimental conditions (L/S = 25, saturated lime solution), and in the presence of gypsum or hemihydrate.

The super saturation degree of the solution can be expressed in function of the activities of the different ionic species in solution and the solubility product, as expressed below:

$$\beta_{ettringite} = \frac{(Ca^{2+})^6 (Al^{3+})^2 (SO_4^{2-})^3 (OH^-)^{12}}{Ks_{ettringite}}$$

$$\beta_{C4AH13} = \frac{(Ca^{2+})^4 (Al^{3+})^2 (OH^-)^{14}}{Ks_{C4AH13}}$$

The results are given in Table 1. When the ionic concentration of the solution increases due to C_3A dissolution, the solution becomes rapidly supersaturated with respect to both AFm and ettringite. These results confirm that under these experimental conditions the ettringite is the least soluble hydrate. Moreover it appears that the solution which leads to the precipitation of hydroxyl–AFm observed within the first minutes of C_3A–gypsum hydration is actually strongly supersaturated with respect to ettringite. Namely $\log\beta_{Ettringite}$ is then at least equal to 12. Nevertheless the early unexpected precipitation of hydroxyl–AFm when C_3A–gypsum hydrates can be due to a difference of the AFm and ettringite nucleation frequency as represented on Fig. 11.

Namely, according to the nucleation classical theory [15,16], the frequency of nucleation increases with the supersaturation degree according to equations (Eqs. (1)–(3)):

$$J = K_0 \exp - \frac{\Delta G^*}{kT} \text{ and } \Delta G^* = \frac{f\Omega^2\gamma^3}{(kT\ln\beta)^2} \quad (1)\text{and}(2)$$

$$\text{and} \quad \Delta G^*_{het} = \Delta G^*\left(\frac{1}{2} - \frac{3}{4}\cos\alpha + \frac{1}{4}\cos^3\alpha\right) \quad (3)$$

and f is a form factor, Ω the volume of the molecule (ettringite or AFm), γ the interfacial crystal solution energy and K_0 a kinetic constant generally comprised between 10^5 and $10^{25}\,cm^{-3}\,s^{-1}$ and α is the wetting angle.

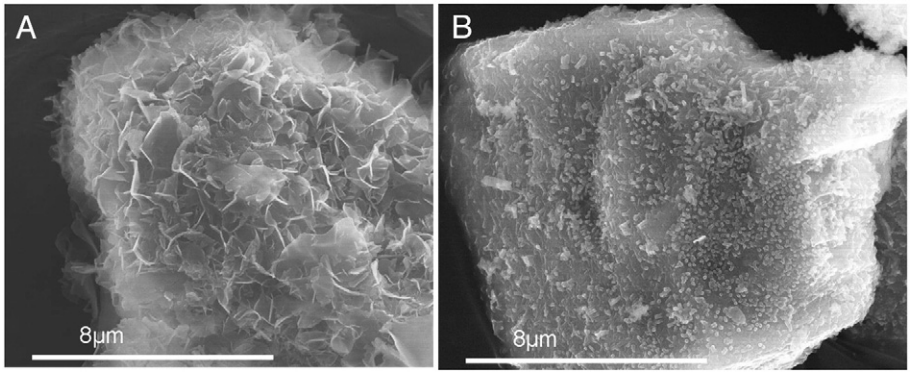

Fig. 10. Micrograph of a grain of C_3A hydrated during 5 min in the presence of (A) gypsum in saturated $Ca(OH)_2$ solution. The C_3A grain is covered by platelets of AFm (B) in the presence of hemihydrate in a saturated portlandite solution. The surface of the grain is covered by small ettringite needles, but no platelet of AFm is observed in this case.

Table 1
Calculation of the super saturation degree attained at the beginning of the C_3A–$CaSO_4$ hydration assuming increasing amounts of dissolved C_3A: under experimental conditions the ettringite is less soluble than AFm.

Gypsum				Hemihydrate			
$[Ca^{2+}] = 27$ mmol/L		$[SO_4^{2-}] = 12$ mmol/L*		$[Ca^{2+}] = 48$ mmol/L		$[SO_4^{2-}] = 26$ mmol/L*	
$C_3A_{dissolved}$ mmol/l	Log β_{Gypsum}	Log $\beta_{Ettringite}$	Log β_{C4AH13}	$C_3A_{dissolved}$ mmol/l	Log β_{Gypsum}	Log $\beta_{Ettringite}$	Log β_{C4AH13}
0.10	−0.02	11.92	−0.20	0.10	0.35	13.62	0.63
0.20	−0.02	12.55	0.43	0.20	0.35	14.22	1.24
0.40	−0.02	13.20	1.11	0.40	0.35	14.83	1.84
0.60	−0.02	13.63	1.54	0.60	0.35	15.18	2.1
0.80	−0.01	13.94	1.87	0.80	0.35	15.43	2.44
1.00	−0.01	14.08	1.98	1.00	0.35	15.63	2.64
2.00	0.00	15.06	3.06	2.00	0.36	16.25	3.25
3.00	0.01	15.52	3.56	3.00	0.36	16.62	3.61
4.00	0.01	15.79	3.82	4.00	0.36	16.88	3.87
5.00	0.01	16.00	4.02	5.00	0.38	17.09	4.07

*$[Ca^{2+}]$ and $[SO_4^{2-}]$ were experimentally determined by ICP-OES.

According to the experimental observations, in the case of the C_3A–hemihydrate hydration, the frequency of ettringite nucleation should accelerate before the nucleation frequency of AFm and consequently ettringite nucleates. On the contrary, in the presence of gypsum, the nucleation frequency of AFm accelerates before the nucleation frequency of ettringite, AFm is then observed before ettringite because, while being less soluble, ettringite has not enough time to nucleate. Fig. 11 shows such a situation.

If it is so, seeding the suspension with ettringite should avoid, at least partially, the precipitation of AFm because under these conditions, the solution has only to be supersaturated for ettringite growth. In order to verify this hypothesis, the same experiments were carried out in the presence of small portion of ettringite crystals. Ettringite was thus added to the initial gypsum suspension in which the C_3A was then added. As previously mentioned (part II) these experiments were carried out using a second batch of C_3A. In order to take into account a possible effect due to the different batches of C_3A, the C_3A hydration was again carried out in the presence of 8% of gypsum and without an initial ettringite addition. Compared to the previous C_3A batch, the new batch of C_3A reacts more slowly in accordance with its lower specific area. Namely the duration needed to consume the gypsum is longer than for the previous C_3A batch (180 min when adding 8% of gypsum instead of 120 min when adding 10% of gypsum with the previous C_3A batch), and the initial heat flow liberated per gram of C_3A is also lower with the new C_3A batch (110 mW instead of 160 mW with the previous C_3A batch).

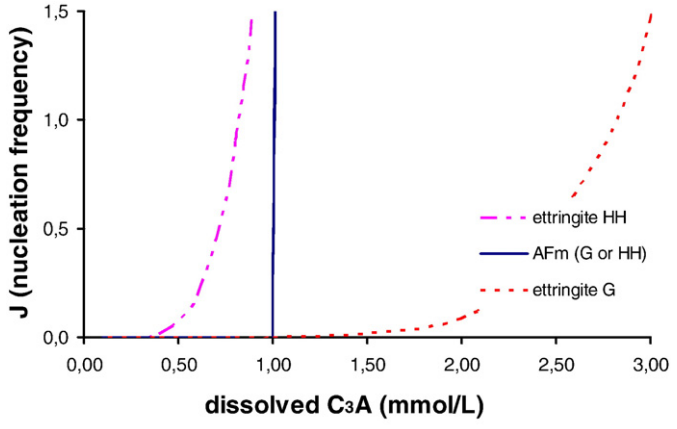

Fig. 11. Increase of the nucleation frequency of AFm and ettringite in function of the amount of dissolved C_3A in the presence of gypsum (G) or hemihydrate (HH). The phase is expected to nucleate instantaneously when the frequency accelerates (for this graph authors used $K_{0\ ett} = 10^{23}\,cm^{-3}s^{-1}$, $K_{0\ AFm} = 10^{20}\,cm^{-3}s^{-1}$, and $\Delta G^*_{het}/kT = 450$ for AFm and 11,000 for ettringite).

The total heat released when sulfate ions are depleted, was again determined by integrating the heat flow curves, and then reported as a function of the initial quantity of added gypsum (Fig. 12). As expected, the slope obtained is again the same as the slopes previously found (Fig. 9).

As previously explained the y-intercept of this curve allows us to estimate the amount of initially-precipitated hydroxy–AFm. It appears that, under these experimental conditions, the presence of ettringite crystals in the initial suspension strongly decreases the quantity of hydroxy–AFm formed at the very beginning of the C_3A–gypsum hydration, because the *y*-intercept is only about 50 J per gram of C_3A under these experimental conditions whereas we estimate that 240 J per gram of C_3A (190 + 50) would have been liberated initially when hydrating this C_3A sample with gypsum but without ettringite addition. This supports the hypothesis that AFm precipitates in preference to ettringite under these conditions mainly because of the slowness of the ettringite nucleation step.

4.2. Ettringite precipitation rate

As far as the kinetics are concerned, in both cases, as expected, the higher the initial quantity of added calcium sulfate, the later the second exothermic peak occurs, meaning that the duration of the ettringite precipitation obviously increases with the amount of calcium sulfate and consequently with the quantity of ettringite formed. However, Fig. 13 shows that for similar amount of added calcium sulfate, the duration of the ettringite precipitation period (hydration period 1) depends on the calcium sulfate form.

Thus the ettringite precipitation rate, which can be deduced from the slope of the curves, strongly depends on the type of calcium sulfate added. If hemihydrate is present in the suspension, ettringite precipitates faster during the first hours of the C_3A–$CaSO_4$ hydration.

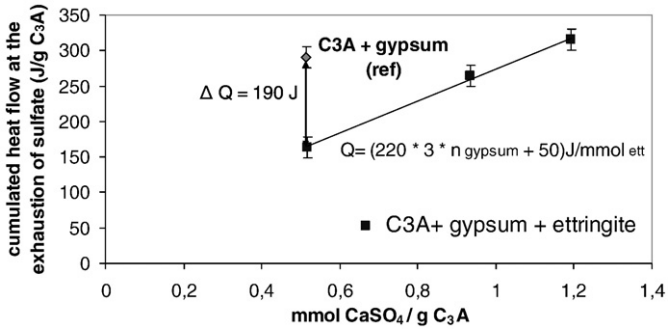

Fig. 12. Cumulative heat flow at the exhaustion of $CaSO_4$ as a function of $CaSO_4$ added; 1 g of C_3A and various amounts of $CaSO_4$ are hydrated in 2 ml of a portlandite saturated solution.

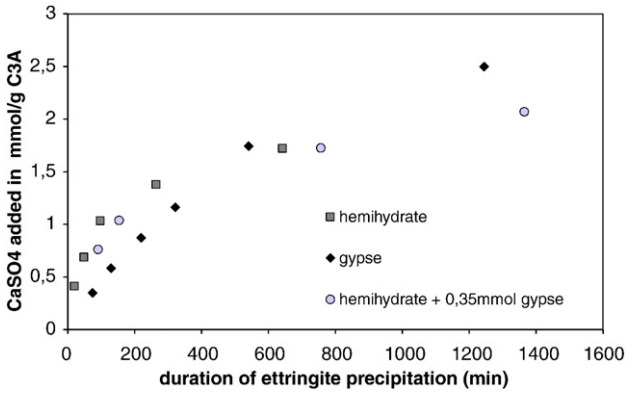

Fig. 13. Effect of the type of added $CaSO_4$ on the duration of hydration period 1 (at L/S = 25). During the first 5 h of C_3A hydration, the presence of hemihydrate leads to a higher ettringite precipitation rate.

This is in agreement with the rate of the ettringite precipitation from C_3A under experimental conditions which can be deduced from the decrease of the sulfate concentration when there is no more solid gypsum in the suspension ($[SO_4^{2-}] < 12.5$ mmol/L). By comparing the slope of both these curves, the rate at which ettringite precipitates from the C_3A seems to be greater in the presence of hemihydrate ($\sim 2 \times 10^{-5}$ mmol ettringite formed per second per gram of C_3A) than in the presence of gypsum ($\sim 1.2 \times 10^{-5}$ mmol ettringite formed per second per gram of C_3A). These results are in agreement with results reported by Bensted [9] showing that during at least the first 2 h of C_3A hydration, the ettringite precipitation rate is higher when gypsum is replaced by hemihydrate. However, when more $CaSO_4$ is added (gypsum >25% by weight of C_3A that is >1.45 mmol/g C_3A) this trend seems to reverse. These curves show that the rate of ettringite precipitation decreases with time, and this effect is more pronounced in the C_3A–hemihydrate system.

This could again result from higher sulfate and calcium concentrations leading to greater supersaturation with regard to ettringite. As previously shown, these conditions favor ettringite nucleation, and if more nuclei are formed, early ettringite formation could be accelerated. Nevertheless, as reported by Gartner et al. [8], the parameters which control the ettringite precipitation rate from C_3A–$CaSO_4$ hydration are still not clear. In such a heterogeneous system, the rate mainly depends on two parameters, the area of the reaction interface and the departure from equilibrium (under- or over-saturation) of the limiting reaction. In this case the limiting reaction could be C_3A dissolution or ettringite precipitation. Several experimental observations tend to show that it is the C_3A dissolution:

- the rate depends on the C_3A specific surface as shown by Brown [2] and Minard [4].
- the aluminium concentration in solution is very low (close to the detection limit) indicating that the reaction imposes the lowest supersaturation degree with respect to ettringite and the highest undersaturation with respect to C_3A.

According to this hypothesis, the high initial consumption of C_3A, corresponding to about 30% of the total C_3A, due to early AFm precipitation, leads to a significant C_3A surface area decrease in the case of C_3A–gypsum hydration that could explain why the initial rate of ettringite formation is lower in the case where the calcium sulfate is gypsum. This could also explain why the intensity of the second exothermic peak, is then lower in the C_3A–gypsum system (~90 mW/g C_3A) than in the C_3A–hemihydrate system (~160 mW/g C3A) which does not initially consume a large part of the C_3A to lead to early AFm precipitation.

However, under these conditions it is difficult to explain why hydration of C_3A–hemihydrate mixtures becomes slower than that of C_3A–gypsum mixtures after 500 min. At this later time the specific surface area of the C_3A is greater in the hemihydrate mixtures, and the undersaturation is the same because all the hemihydrate has by then converted to gypsum.

In the case of the second hypothesis, ettringite precipitation should be the limiting step. The greater rate in the presence of hemihydrate could then result from a greater number of ettringite nuclei that is generally obtained when the supersaturation is higher. The decrease of the rate after 500 min could then result from a reduction of the surface growth of ettringite due to the coalescence of neighbour nuclei.

In order to evaluate the contribution of this surface effect, the same experiments should be carried out on monodisperse C_3A grains, but under the experimental conditions it is difficult to properly take into account of the surface effect.

5. Conclusions

This study showed that the composition of the initial hydration solution is the relevant parameter which controls the early fast C_3A hydration: while under the experimental conditions, early C_3A–gypsum hydration carried out in a calcium hydroxide saturated solution gives rise to both hydroxy–AFm and ettringite precipitation, the presence of hemihydrate prevents the more soluble hydroxy–AFm from precipitating within the first minutes.

Under experimental conditions, the early hydroxy–AFm precipitation is strongly decreased when small amounts of ettringite are added to the C_3A–gypsum system proving that the ettringite nucleation is the limiting step of the early ettringite precipitation.

This study shows that higher super saturation degrees and then higher nucleation frequency with regard to the ettringite are obtained in the presence of hemihydrate, this explains why the early hydroxy–AFm precipitation is avoided as soon as hemihydrate is added. Concerning the ettringite precipitation rate, we also confirmed that replacement of gypsum by hemihydrate leads to an increase of the ettringite formation rate during at least the five first hours under our conditions.

Consequently the sulfate type used is expected to strongly modify the early C_3A–$CaSO_4$ hydration products and the rate of this hydration. This undoubtedly will have further effects the rheology of the fresh paste.

Acknowledgements

The authors are grateful to Philippe Maitrasse and Bruno Pellerin from Chryso and Sebastien Georges from Lafarge who supported this study and to Ellis Gartner from Lafarge for his helpful comments. They also would like to thank Daniele Perrey from ICB, and Isabelle Baco from Lafarge for their help during calorimetry experiments and dosages.

References

[1] H.F.W. Taylor, Cement Chemistry, 2nd ed., Thomas Telford, 1997, edition.
[2] P.W. Brown, L.O. Libermann, G. Frohnsdorff, Kinetics of the early hydration of tricalcium aluminate in solutions containing calcium sulfate, J. Am. Ceram. Soc. 67 (1984) 793–795.
[3] W. Eitel, Recent investigations of the system lime–alumina–calcium sulfate–water and its importance in building research problems, J. Am. Res. Inst. 28 (1957) 679–698.
[4] H. Minard, S. Garrault, L. Regnaud, A. Nonat, Mechanisms and parameters controlling the tricalcium aluminate reactivity in the presence of gypsum, Cem. Concr. Res. 37 (2007) 1418–1426.
[5] F.J. Tang, E.M. Gartner, Influence of sulphate source on Portland cement hydration, Ad. Cem. Res. 1 (2) (1988) 67–74.
[6] J. Skalny, M.E. Tadros, Retardation of tricalcium aluminate hydration by sulfates, J. Am. Ceram. Soc. 60 (1977) 174–175.
[7] R.F. Feldman, V.S. Rachamadran, The influence of Ca2SO4. 2H2O upon the hydration character of CaO. Al2O3, Mag. Concr. Res. 57 (1966) 185–196.
[8] E.M. Gartner, J.F. Young, D. Damidot, I. Jawed, Hydration of Portland cement, in: J. Bensted, P. Barnes (Eds.), Structure and Performance of Cements, 2002, pp. 57–113.
[9] J. Bensted, Effects of the clinker–gypsum grinding temperature upon early hydration of Portland cement, Cem. Concr. Res. 12 (1982) 341–348.

[10] E. Sakai, J.K. Kang, M. Daimon, Influence of superplasticizers on the very early hydration of $Ca_3Al_2O_6$ in the presence of gypsum, $CaSO_4$ $0.5H_2O$ and CaO, Cem. Sci. Concr. Technol. 56 (2002) 36–41.
[11] R. Barbarulo, H. Peycelon, S. Leclercq, Chemical equilibria between C–S–H and ettringite, at 20 and 85 °C, Cem. Concr. Res. 37 (8) (2007) 1176–1181.
[12] W. Lerch, The influence of gypsum on the hydration and properties of Portland cement pastes, in Proceedings, American Society for Testing Materials: Bull, vol. 12, 1946, pp. 1–41.
[13] H. Minard, Etude intégrée des processus d'hydratation, de coagulation, de rigidification et de prise pour un système C_3S–C_3A–sulfates–alcalins, in Université de Bourgogne. 2003: Dijon France.
[14] D. Damidot, F.P. Glasser, Thermodynamic investigation of the calcia–alumina–calcium sulfate–potassium oxide–water system at 25 C, Cem. Concr. Res. 23 (5) (1993) 1195–1204.
[15] A.E. Nielsen, O. Sohnel, Interfacial tensions electrolyte crystal aqueous solution from data, J. Cryst. Growth 11 (1971) 233–242.
[16] R. Boistelle, Concepts de la cristallisation en solution. Actualités néphrologiques, in: J. Crosnier, et al., (Eds.), Flammarion Médecine Science, 1985, pp. 159–202.